Renewable Energy-Based Electric Drive with a Novel Control Technique for Smooth Power-Sharing

RAKESH BABU BODAPATI*, R. S. SRINIVAS, P. V. RAMANA RAO
[1]Department of Electrical and Electronics Engineering,
Acharya Nagarjuna University,
Guntur, Andhra Pradesh-522510,
INDIA

**Corresponding Author*

Abstract: - Energy management between different power sources, which are used to feed Electric vehicles (EVs) is one of the complex scenarios. Normally, power management is done based on the Electric vehicle load requirements. In this work, three different energy sources are considered, in that one is an active energy source and two are passive energy storage elements. The Photo Voltaic (PV) based energy source is considered an active element, on the other hand, the Battery sand supercapacitor (SCap) is treated as a passive type of element. To manage the power flow between two energy sources, a novel control technique is adopted by considering the speed and current of the electric motor as major input parameters known as the Measurement of the parameter-based controller (MPBC). The Measurement of a parameter-based controller is used to control the pulse signals of the Bidirectional converters connected at the battery and supercapacitor ends, and the required pulse signals can be generated by the Conventional Proportional Integral (PI) controller. The main circuit is implemented with a novel hybrid controller which is used to provide controlled pulse signals to the bidirectional converters connected to the battery and supercapacitor. Finally, the MATLAB/Simulink model was developed with the novel hybrid controller and examined the performance at different load conditions of the motor by considering three different states of power delivered by the PV array.

Key-Words: - Electric vehicle, Battery, Photo Voltaic (PV) energy, Energy Management (EMGT), Proportional Integral (PI) controller, Hybrid controller (HC), Measurement of parameter-based controller (MPBC).

Received: March 17, 2024. Revised: August 9, 2024. Accepted: September 9, 2024. Published: October 22, 2024.

1 Introduction

In the coming days, Renewable energy (RE) sources become the main source to develop electricity rather than other conventional energy sources. Since the conventional energy-based electricity generation becomes costlier and will affect badly on the environment due to huge emissions. To produce energy cheap and environment-friendly, the main alternating solution is solar-based power generation. Here solar-based power can be produced by taking sunlight and irradiance as an input which is available abundantly, without paying any cost to nature. During the production of power using solar-based plants, no considerable emission will be generated in the atmosphere, which shows the environmentally friendly nature.

Nowadays a major part of transport is done by using the conventional vehicle system only. However, this conventional vehicle system-based transport system needs to be changed based on the input energy storage system used. Normally in a conventional transport system vehicle's energy source is petrol or diesel which are limited in nature and also produce a huge number of exhaustive gases during the operation of the vehicle. To overcome future scarcity in conventional fuels, need to switch to another alternating source-based vehicle. Battery-based electric vehicles are developed instead of Internal combustion engine-based vehicles, to reduce petrol/diesel usage. Generally, to charge the Battery we need to plug in the vehicle for complete charging of the energy source. This factor again leads to putting the burden on the local power grid. To avoid a burden on the local grid separate power generation station is made within the vehicle itself using a solar-based power plant. This will reduce the load burden on the local power grid.

1.1 Literature Review

Renewable energy sources like solar, biomass, and wind are generating power by taking input from abundantly available sources. For example, sunlight is available all the way in day times with this, increasing load demand can easily be met without any dependency. As per the standard survey results, more than 70% of power generation can be done using conventional methods. On the other, max 30% of power is only generated using a renewable resource. This is not a good sign for the environment. This non-conventional power generation should be increased to the maximum possible extent by educating the people in society. This effort will increase the use of EVs from a transportation point of view and reduce the burden on the local grid, [1].

Since fossil fuels are being depleted rapidly, alternative sources of energy are needed urgently to meet the current load demand. The use of fossil fuels is also accountable for global warming trends, [2]. To address this global energy crisis, renewable energy sources are the most viable option. RE sources are expected to play a pivotal role in supplying the future's electricity, [3], [4].

Study of combined real-time load development and energy storage management at grid-associated solar EVs. Deprived of any earlier expertise, a finite time method has been considered with subjective dynamics of structure inputs. The purpose is to reduce a standard aggregated system price through combined optimization of EV's energy ordering amount, load planning delays, photovoltaic abundance in times of nearby produced renewable energy, and battery deprivation. Because of successive adjustment and reformulation of the combined optimization challenge, the model of one-slot look-ahead queue stability to solve the difficulty by utilizing the Lyapunov optimization method (LOM), [5].

For enhanced energy consumption, the selection of HEVs in transport systems is more attractive and more pronounced. The HEVs are achieving vast growth due to their eco-friendly implementation and support of the smart grid concept. The difference of ESS in HEV with several control approaches creates variant in HEV types. This enables, selecting an applicable control strategy for HEV uses to become difficult. A thorough review of the vital information of ESS related to HEVs and obtainable optimization topologies based on different control schemes and vehicle tools, [6].

In this, as a part of the investigation and analysis, the transformation of the traditional vehicle system is converting into self-sustainable EVs. During this process, reach out to several ESS devices like lead-acid batteries and lithium-ion (Li-ion) batteries. MATLAB/Simulations have been carried out utilizing three driving cycles that correspond to the conditions of moving in: a highway with a climb of mountain and city, a highway, all requirements being based on roads in the Vale do Paraíba Paulista region, [7], [8].

In this work, to diminish the power density scarcity of current ESS in EVs and HEVs, which comprises a battery and a supercapacitor, is respected. Energy management has to be taken out for the HESS due to the presence of the two ESSs. By considering, Pontryagin's minimum principle the finest energy management approach is developed, which immediately allocates the mandatory impulsion power to the two ESS during the vehicle's propulsion and also immediately assigns the regenerative braking energy to the two ESS, [9].

Developing a supervisory control technique, for HESS-based EVs is the main challenge for optimized energy management. Multi objectives-based optimization model is formulated for improved power exchange between the battery and the supercapacitor. This technique works optimally and resolves in a systematic way of approach, [10], [11].

Using a nonlinear control system method, a real-time combined speed control and power flow supervision system is created for an EV powered by supercapacitors. This work adopts a controller design for HESS sizing to determine optimally the size of HESS to serve an EV given the coupling between energy management and HESS sizing. To decrease battery stress, the controller traces the vehicle's set speed with universally exponential stability and wisely uses the HESS to diminish power utilization. A composite controller is required by utilizing the physical origin of the vehicle's power demand. A full-size EV's driving cycle is simulated on a standard urban dynamometer driving program to determine the usefulness of the controller and HESS sizing system, [12]. This work aim of this work is to identify $2n - 1$ stage rearrangeable banyan-type networks that are not isomorphic to each other. This is accomplished by creating alternative networks and using the satisfiability issue to assess how well they can be rearranged. Due to the large number of candidates, this approach's low scalability is a disadvantage. It is demonstrated that the possibilities can be reduced to a smaller set of networks known as pure banyan networks to get rid of this problem. Network isomorphism analysis is used to accomplish this, [13], [14]. By thoroughly reviewing the Moroccan

hydrogen roadmap, this study aims to bring insight into fuel cell electric vehicles and investigate the prospects for FCEV use in Morocco. A SWOT analysis was also conducted to identify the critical success element for promoting FCEV adoption in the Kingdom, [15], [16]. The study presented application scenarios, including power output fluctuations reduction, output plan acceptance at the renewable energy generation side, power grid frequency adjustment, power flow optimization at the power transmission side, and a distributed and mobile energy storage system at the power distribution side, based on an analysis of the development status of a BESS, [17], [18], [19], [20].

2 Configuration of the Existed Model

Figure 1 shows the existing model configuration with two sources in that one will act as a main source and the other will act a main source. In this battery used as the main source, the supercapacitor is used to meet the sudden power requirements. Two Bidirectional converters are used here for two energy sources. The speed (W), load torque (T), and driver commands are the main inputs to the central control to develop the pulse signals to the convert based on the load requirement. The main drawback of this model is no permanent setup is available at the vehicle end to charge the energy sources. Hence this type of configuration requires standalone charging station, which again will cause trouble on the local grid system during the charging period of the electric vehicle. Overall system setup requires two converters, and two energy sources which leads to more cost during real-time implementation.

The supercapacitor used in this system is not a cost-effective device compared to the battery, but this is required as per the designed configuration to supply peak power during abnormal conditions like cold start, sudden stop, and start conditions on the electric vehicle.

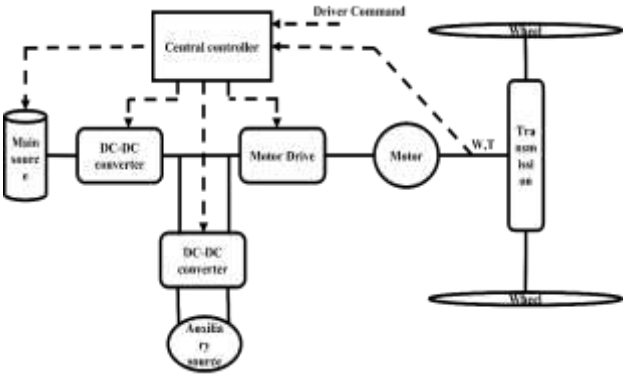

Fig. 1: Existed model of Electric vehicle with multiple sources and converters

In this arrangement single central controller is used to provide the controlled signals to the converters due to this there is a delay happens during giving signals to the drive command.

The present work used only one energy source with inbuilt power generation with solar energy to generate power vehicle itself without depending on the local power grid. With this arrangement, the EV can develop power with solar panels when sunlight is available and parallelly able to charge the battery. Which is used full during nighttime driving situations, which means the battery will provide the necessary power to the load for continuous operation.

2.1 Battery Model

Figure 2 shows the Parameter auto partner Programme PNGV Model of the battery. a large capacitor C1 is added in the main Thevenin's circuit model.

The differential equations related to the PNGV battery model are represented as, R1 is the ohmic resistance of the battery, VLoad is the terminal voltage, Vopen ideal voltage source, I(t) charge discharge current, R2 is the nonlinear contract resistance, C2 is electrode plate equivalent capacitance, IR2(t) current through nonlinear resistance R2, IC2(t) Current through electrode plate capacitor, V1 Voltage across capacitor C1, V2 Voltage across capacitor C2.

$$V_{Load} = V_{Open} - i(t) * R_1 - V_2 - V_1 \quad (1)$$

$$V_2 = \frac{-V_2}{R_1 C_1} + \frac{i(t)}{C_1} \quad (2)$$

$$V_1 = C_1 \int i(t) dt \quad (3)$$

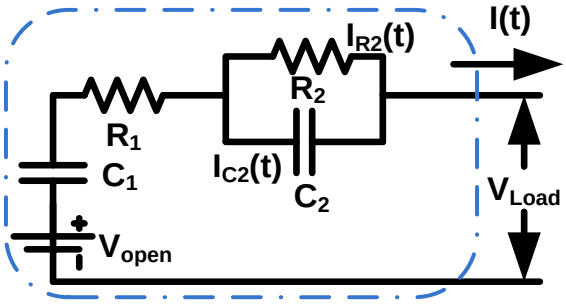

Fig. 2: PNGV Model of the Battery

2.2 Modeling of Practical PV Module and Array with PV Cell

All cells are simultaneously connected to series and shunt resistances in practice since there is no ideal

cell. Parallel resistance is caused by leakage current, while series resistance is caused by hindrance in electron flow from n to p junctions. The model is generalized to consider the losses due to series, shunts, and recombination. A photovoltaic cell in practice is shown in Figure 3.

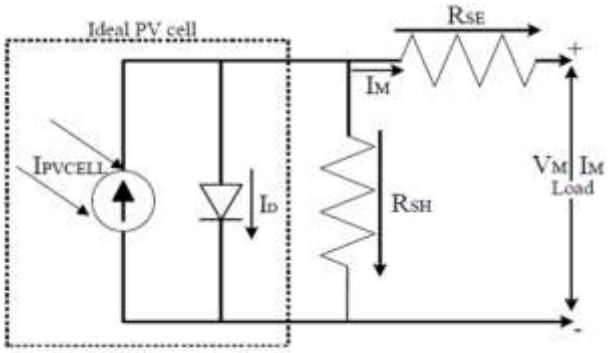

Fig. 3: Equivalent electric model of the PV array
Kirchhoff's current law (KCL) says that PV cells produce an output current of IM

$$I_M = I_{PVCELL} - I_D - I_{SH} \quad (4)$$

Where:
PV output current is expressed in amps as IM

The diode current in amps is called ID and Shut resistance is the resistance across which ISH is measured.

Since the practical cell contains additional resistances, the effects of the resistances must also be considered. Modules are made up of PV cells, and arrays are made up of modules and arrays are made up of PV cells. PV modules are constructed by connecting 60 PV cells in series and parallel. Therefore, 10 cells are linked in series, and these six combinations are linked in parallel. For charging a 12 V battery, a 36 cell PV module provided the required voltage, and similarly for charging a 24 V battery, a 72-cell solar PV module was used. Photovoltaic systems are commonly used with batteries to provide backup power. In this case, however, 60-cell PV modules are used.

3 PI+MPBC Energy Management Strategy

In this, a novel control technique is proposed to make the switching between charging and discharging states of the battery, and SCap based on the speed and current values of the electric motor. To achieve the proposed control technique two different controllers are selected in that, PI is a traditional controller that is used to generate the pulse signals to the converter. An MPBC controller is used to regulate those signals based on the speed and current values of the electric motor. Finally, this combination of MPBC+PI provides a way to meet the proposed methodology.

3.1 Main Circuit with Novel Control Strategy

In the proposed model the main circuit includes a PV array, Battery, SCap, two bidirectional converters, Boost converter, and the electric motor represented in Figure 4. Here battery is used to provide backup power to the EV during unavailable Solar power generation situations on the other hand SCap is used for to meet the peak power requirement. Whereas a PV array is used to meet the EV requirement and also for battery and SCap charging depending upon the load applied to the EV. All the controlled signals of the two Bidirectional converters are controllers based on the Proposed control technique which includes two individual controller combinations named as MPBC plus PI. Here PI controller is used to generate the pulse signal to the converter at the battery and SCap end based on the actual and reference voltage values of the converter. On the other hand, MPBC works based on the current and speed values of the EM, and this can be done with math functions which will generate three different types of signals based on the current and speed values of the EM. Finally, the combination of MPBC and PI works to provide controlled pulse signals to the converter at battery and SCap ends, which leads to providing proper power supply to the EV as per the applied load.

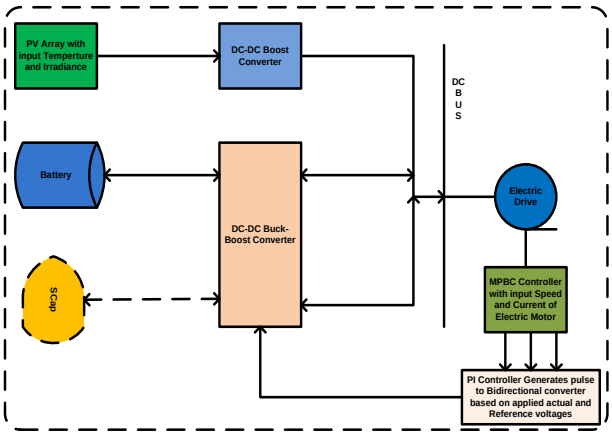

Fig. 4: Main circuit with a Proposed control technique

Here three different load conditions are considered and based on these, the controlled signals will be generated to the EV. This will

happen as per the proposed controlled technique which is the combination of MPBC plus PI.

The math functions generation related current and speed of the EM as discussed.

1. If the speed is greater than or equal to 1500 rpm and the current is less than 6A then MPBC generates a signal as 1 for Y1 and zero for remain two functions Y2 and Y3. Due to this the converter at the battery end and SCap will work under buck mode and the battery, SCap (shot period) gets charged from solar energy. The current will flow from the PV array to the battery, SCap (for a short period), and Load. Even SCap will discharge the same amount of energy if the load on the motor is huge during starting.
2. When the speed is between 1400rpm and 1499rpm and the current value lies between 6A to 8A then the proposed controller MPBC will generate signals as one for math function Y2 and zero for the remaining two functions. In this case, there is no operation required from the converter at the battery end and SCap will provide the necessary peak power to the motor in a short period with this the converter at SCap will work under boost mode. The current will flow from the PV array plus SCap (short period) to the load and no current will flow to the battery. This means in this case battery neither charged nor discharged.
3. If the speed of the EM is less than 1400 rpm and the current is greater than 8A the MPBC will generate signal as one for Y3 and zero for the other two functions. With this the converter at the battery and SCap end worked under boost mode, hence the current flows from the battery, SCap (for a short period), and PV array to load. This indicates that during huge load conditions, Battey is assisting the PV array along with the SCap till the end of the charging.

$$X(\mathrm{t}) = \mathrm{Y}_1 \mathrm{When, Speed} \geq 1500\,\mathrm{RPM} \&\& \mathrm{Current} < 6\,\mathrm{A} \quad (5)$$

$$X(\mathrm{t}) = \mathrm{Y}_2 \mathrm{When, Speed} > 1400\,\mathrm{RPM}, \& < 1499\,\mathrm{RPM} \&\& \mathrm{Current} > 6\,\mathrm{A} \& < 8\,\mathrm{A} \quad (6)$$

$$X(\mathrm{t}) = \mathrm{Y}_3 \mathrm{When, Speed} < 1400\,\mathrm{RPM} \&\& \mathrm{Current} > 6\,\mathrm{A} \quad (7)$$

Here
X(t) is the final output function of the MPBC controller
Y1 is the math function 1 output of the MPBC controller
Y2 is the math function 2 output of the MPBC controller
Y3 is the math function 3 output of the MPBC controller

All three modes of operation of the circuit with proposed model is represented in Figure 5.

3.2 Power Calculations Related to Energy Sources

These calculations are done based on the two passive elements used in this work and the PV array is the active and main source of producing the energy.

3.2.1 Battery

Before calculating the specific application-related rating of the motor needs to consider and know the cell voltage, ampere hour rating, and the C rate of the battery. Normally cell voltage means the nominal voltage only comes under consideration, the AH of the battery determines how much current can be delivered within one hour, and the C rating of the battery denotes the charging and discharging time.

For a maximum speed 1600 rpm the current drawn by the motor is calculated by using

$$\frac{V * AH}{1000} = Motorcapacity = 1Kw \quad (8)$$

$$AH = \frac{1000}{160} = 6.25Amp \quad (9)$$

To get the fruitful operation of the Motor in all road conditions need to consider the acceleration current (consider 5% more than the actual one) and then the effective current value as:

$I_{effective}$=6.25*0.05+6.25=6.5625Amp

Then we know that the power equation:

$$P_{Batt} = V_{Batt} * I_{Batt} \quad (10)$$

Then the power required at 1600 rpm of the motor is:

$$P_{Batt} = 160 * 6.5625 = 1050Watts \quad (11)$$

3.2.2 Supercapacitor

The power capacity of the supercapacitor is given as:

$$P_{SCap} = P_T - P_{Batt} \quad (12)$$

Here PScap is the power capacity of the SCap

PT is the total power demand
PBatt is the battery capacity
From the equivalent series resistance model of the SCap we know the equation:

$$\frac{1}{2}C_{SCapmin}\left(V_{SCapNom}^2-V_{SCapmin}^2\right)=P_{SCap}d \quad (13)$$

Generally, VSCapmin is chosen as VSCapmax/2 from equation xx which shows that 75% of energy is utilized from the full charge. When the SCap voltage reaches to bottom limit VSCapmin stops working and gets charged to maintain SOC to avoid stress:

$$P_{SCap}(t)=V_{SCap}(t)*i_{SCap}(t)=1000Watts \quad (14)$$

$$V_{SCapnom}=36V$$

$$V_{SCapmin}=\frac{1}{2}V_{SCapnom}=18V$$

The continuous discharge time is $t_d=10\sec$

Then $$C_{SCapmin}=\frac{2P_{SCap}t_d}{V_{SCapnom}^2-V_{SCapmin}^2} \quad (15)$$

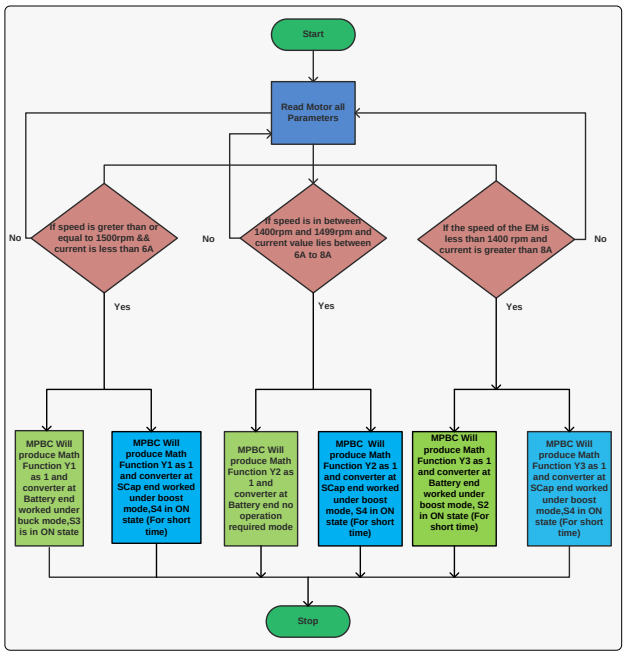

Fig. 5: Represents how the proposed control technique works

3.3 Modes of Operation of the Main Circuit Model

The complete operation of the main circuit is divided into three modes based on the load applied to the EV. Figure 6, Figure 7 and Figure 8 are related to different modes of operation of the main circuit about the applied load.

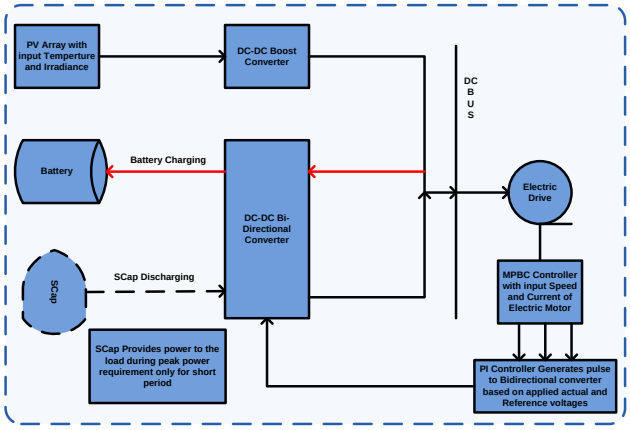

Fig. 6: The main circuit with load and battery power meet from the PV array and SCap short time

Figure 6 shows the main circuit with normal load conditions on the EV. In this case, the PV array is capable of supplying power to load as well as the battery for its charging. This indicates that, based on the speed and current values of the EV, the controlled pulse signals are generated to the converter at the battery end to work under the buck mode of operation. Here the converter at the PV array end always works under the boost mode of operation. This shows that the MPBC controller will be able to generate the signals as 1 for math function Y1 and zero for remaining two functions. Along with this, the SCap supports the PV array during peak power conditions on the electric motor, which means the SCap is exclusively meant for peak power requirements.

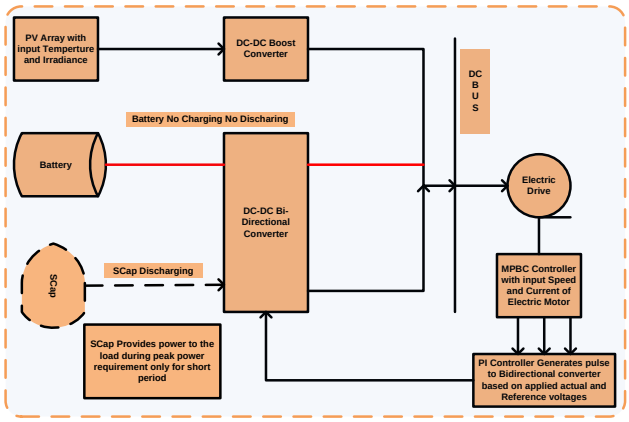

Fig. 7: The main circuit with load power meet from the PV array and SCap for a short time

Figure 7 represents the main circuit power flow from the PV array to EV only due to the rated load applied to the EM. In this case, the pulse signals generated by the PI are controlled by the MPBC controller as per the proposed control technique. Hence the MPBC will develop Y2 function as 1 and zero for remaining math functions. In this mode of

operation, the converter at the battery is under no working zone, which means the battery is neither charged nor discharged. Along with this, the SCap supports the PV array during peak power conditions on the electric motor.

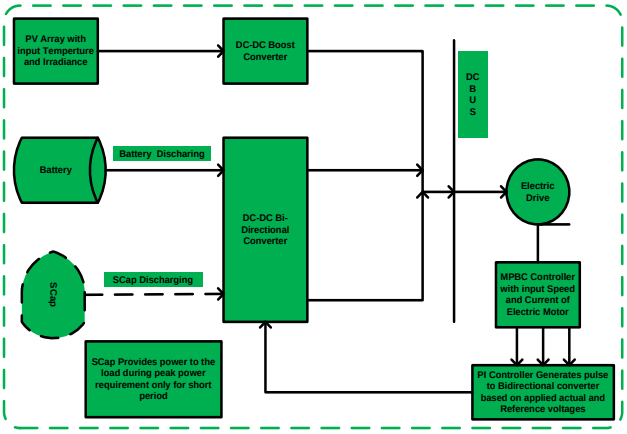

Fig. 8: The main circuit with load power meets from the PV array and battery

Figure 8 demonstrates the Main circuit current flow from the PV array plus the battery to the load. This shows the high load applied to the EV, because to battery supports the PV array by providing extra power to the power to load as per the requirement. The MPBC controller can generate the signal as 1 for math function Y3 and zero for the remaining two functions Y1, Y2 due to which the PI generated pulses are controlled and provided to the converter at the battery end to perform the boost operation only. Along with this, the SCap supports the PV array during peak power conditions on the electric motor, and converter works under boost mode.

4 Simulation Result and Analysis

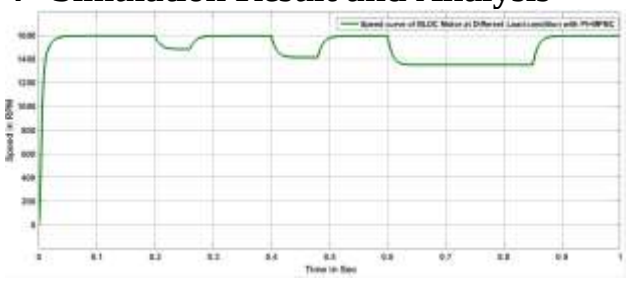

Fig. 9: Speed curve representation of electric motor at different load conditions

The speed curve response of EM with different loads are represented in Figure 9. Here three different loads are applied at different periods to the EV to verify the effectiveness of the proposed control technique. At 0.2 sec normal load is applied to the EM, which leads to a decrease the speed of the EM approximately equal to 1500rpm, at 0.4 sec rated load is applied due to this the speed of the motor reduces further to 1400rpm and at 0.6 sec more that rated load is applied this causes speed reduction further less than 1400rpm. Corresponding to all corresponding applied loads the current also increases.

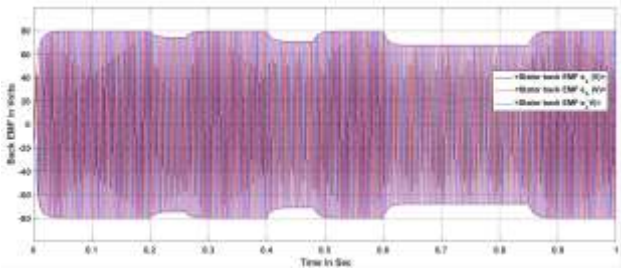

Fig. 10: Back EMF of the electric motor at different load conditions

Figure 10 shows the Back EMF curve of the electric motor with different load conditions. This will follow the speed curve at 0.2 sec the curve seems to decrease and after some time reaches the steady state, thereafter at 0.4 sec rated load condition on the EM the back emf reduces for some time and reaches again steady state. Finally at 0.6 sec again the back emf value is reduced drastically due to more than rated load applied to the motor, it will continue for some time thereafter it will reach again a steady state value, all this happens because of the proposed control technique.

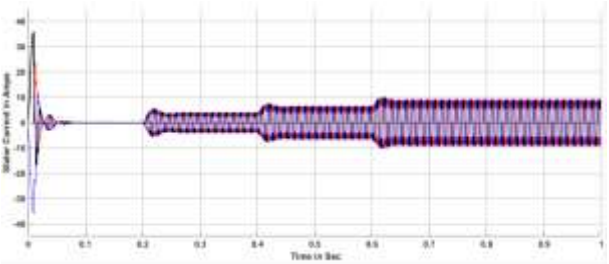

Fig. 11: Electric motor current changes related to load

Electric motor current at different load conditions can be represented in Figure 11. Initially, the current drawn by the motor is huge and, after reaching a steady state that value becomes nominal which means, the motor is working under no load condition. At 0.2, 0.4,0.6 sec different kinds of load are applied to the EM which leads to an increase the current drawn by the motor as per the applied load, those values are 6A,8A, and more than 8A. For the first two cases, the PV array only meets the load requirement, and in the third case PV array and battery together supply power to the load. In all the

modes of operation, SCap will provide power during the peak power requirement, especially at sudden load changing conditions on the electric motor.

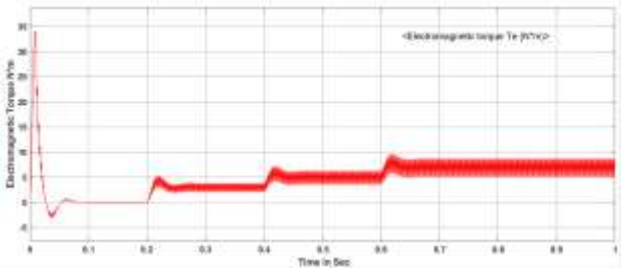

Fig. 12: Load changes representation on the Electric Motor

Figure 12 shows the load curve representation on the EM. Before reaching a steady state, the motor is with huge load due to which EM will take more current than regular intervals. At 0.1 sec onwards the motor reaches a steady state so no load will appear in the motor which is very clear from Figure 12. To know the performance of the proposed control technique different loads are applied at 0.2,0.4 and 0.6 sec due to which the current drawn by the EM increases parallelly the speed of the motor decreases.

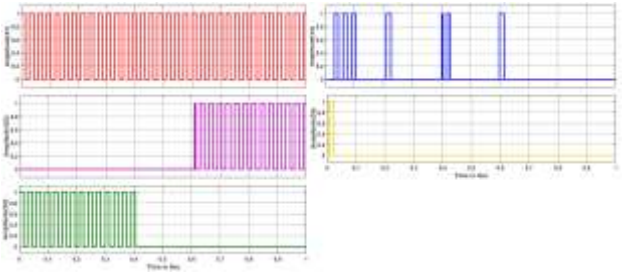

Fig. 13: Pulse signals representation of Switches S1, S2, S3, S4, and S5 corresponds to load conditions on the electric motor

Pulse signals representation corresponding to the three switches present in two converters at the battery, PV array ends shown in Figure 13. The switches S2, and S3 are related to the converter at the battery end which will perform both boost and buck operations depending upon the load requirement as per the proposed controlled technique. At the same time, S1 is the only switch related to the converter at the PV array end which is used to work the converter under boost operation always. Figure 13 clearly shows that the pulse signals to the S1 are always in ON state which indicates that the PV array is always providing power to the load some to the battery also depending upon the load applied condition. For S3 the pulses will be present from 0 to 0.41 sec which indicates the charging period of the battery from the PV array. From 0.41 to 0.6 sec no pulses are provided to the S2 and S3 this indicates that the converter at the battery is not required during this period. From 0.6 sec to 1 sec the pulses of S2 and S1 are present which shows that the battery and PV array combine meeting the load requirement of the EM. In addition to that the SCap is capable of providing peak power to the electric vehicle, especially at sudden load change conditions and starting of the motor. Here Switches S4 and S5 are related to the converter connected at the supercapacitor end. These two switches are useful for the charge and discharge of the SCap as per the load requirements and power availability from the source. From Figure 13 it is clear that switch S4 is for discharging the power to the load during sudden load changing on the motor whereas switch S5 is used for buck mode of operation.

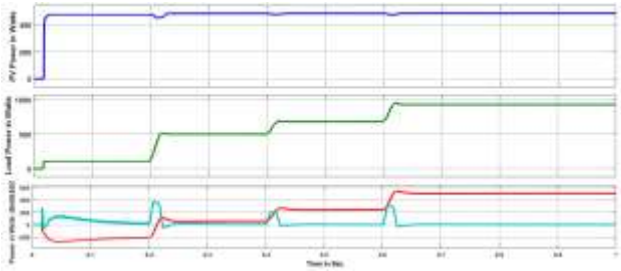

Fig. 14: Power curve representation of the PV array, Load, battery, and SCap

Figure 14 shows the, power curves of the PV array, Load, SCap, and the battery. Here the PV array can develop the power continuously to the load as per the available temperature and irradiance as input to the PV array. From 0 to 0.4 sec the power required by the load is supplied by the motor and battery charging is supplied by the PV array. From 0.4 to 0.6 sec the also PV array alone provides power to the load and zero power absorbed by the battery. From 0.6 sec onwards the power required by the load is met by the PV array and the battery. In addition to that the SCap provides power to the load at 0.01 to 0.1 sec, 0.2 sec, 0.4 sec, and 0.6 sec during sudden load changes on the electric motor.

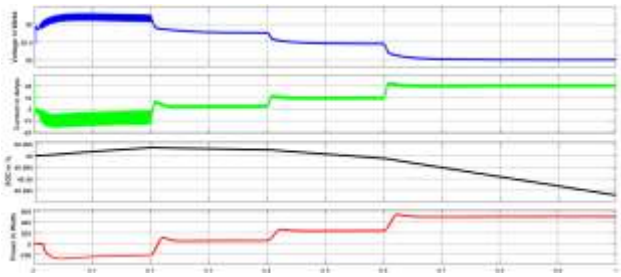

Fig. 15: Battery parameters representation

Battery Voltage, current, %SOC, and Power curve of the battery are shown in Figure 15. The voltage curve shows that the value is in a decreasing manner depending upon the applied load on the EM. From 0 to 0.4 sec battery is in charging modes which clearly shows from the current curve of the battery indicating a negative value and in the same way %SOC of the battery also increased to 0.4 sec there after maintained a flat value up to 0.6 sec. From 0.6 sec on words the current value becomes positive and SOC value decreases and the Power value, all this happens as per the load applied to the EM.

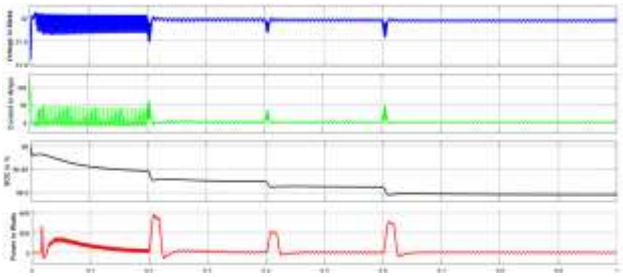

Fig. 16: Supercapacitor parameters representation

The SCap related parameters are shown in Figure 16, which indicates that the voltage value drops at 0.2 sec, 0.4, and o.6 sec corresponding to this the current value of SCap also raised and the power also obtained for a short period which is required to during sudden load changing on the electric motor.

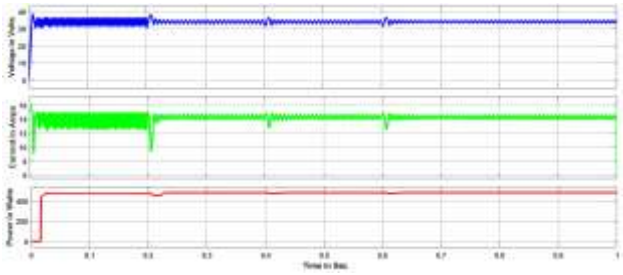

Fig. 17: PV array parameters representation

Figure 17 shows the PV array curves which include Power, current, and voltage values. This shows that all values related to the PV array maintain the content value throughout the operation.

5 Conclusion

A novel control technique was developed to meet the electric vehicle requirement as per the applied. The speed current condition-based controller was developed with three math functions Y1, Y2, and Y3. There the modeled controller is combined with proportional integral is combined with to achieve the proposed control technique. The three math functions output will decide the operation of the converter at the battery and SCap end, if the Y1 value becomes 1 then the converter at the battery works under buck mode, in the same way, if Y3 becomes 1 the same converter works under boost mode and finally if Y2 becomes 1 then no operation is required from the bidirectional converter, all this happens based on the load applied to the Electric vehicle. To verify the effectiveness of the proposed control technique three different load cases are considered, in the first case normal load is applied due to which the speed of the motor reduces up to 1500rpm parallel current increases to 6A, due to this the speed current condition-based controller produces signal as 1 for Y1 and zero for Y2 and Y3, which makes the operation of the converter at battery end as a buck. In the same way, the motor speed reduces to up to 1400rpm due to the rated load applied to the motor in the second mode of operation. This leads to generating the math function Y2 as 1 from the speed current condition-based controller due to this no operation is required from the bidirectional converter. Finally, in the last case more than the rated load is applied to the motor due to which the speed of the electric motor reduces to less than 1400rpm, and the current value is more than 8A which leads to producing Y3 as 1 from speed current condition-based controller, due to this the converter at battery end works under boost mode of operation. In addition to that the SCap side converter works under boost mode during all sudden load changes happens on the electric motor, to provide the required peak power of the load. In this way, the effectiveness of the proposed control technique using speed current condition based on proportional integral derivative controller was verified with different load conditions on the electric vehicle in MATLAB/Simulink Environment.

References:

[1] Qazi, A., Hussain, F., Rahim, N. A., Hardaker, G., Alghazzawi, D., Shaban, K., & Haruna, K. (2019). Towards sustainable energy: a systematic review of renewable energy sources, technologies, and public opinions. *IEEE access*, 7, 63837-63851.

[2] Rehman, W. U., Bhatti, A. R., Awan, A. B., Sajjad, I. A., Khan, A. A., Bo, R., ... & Oboreh-Snapps, O. (2020). The penetration of renewable and sustainable energy in Asia: A state-of-the-art review on net-metering. *IEEE Access*, 8, 170364-170388.

[3] Gielen, D., Boshell, F., Saygin, D., Bazilian, M. D., Wagner, N., & Gorini, R. (2019). The role of renewable energy in the global energy transformation. *Energy strategy reviews*, 24, 38-50.

[4] Katuri, R., & Gorantla, S. (2020). Realization of prototype hardware model with a novel control technique used in electric vehicle application. *Electrical Engineering*, 102(4), 2539-2551.

[5] Ahmad, A., & Khan, J. Y. (2019). Real-time load scheduling and storage management for solar powered network connected EVs. *IEEE Transactions on Sustainable Energy*, 11(3), 1220-1235.

[6] Podder, A. K., Chakraborty, O., Islam, S., Kumar, N. M., & Alhelou, H. H. (2021). Control strategies of different hybrid energy storage systems for electric vehicles applications. *IEEE Access*, 9, 51865-51895.

[7] dos Santos, G. S., Grandinetti, F. J., Alves, R. A. R., & de Queiróz Lamas, W. (2020). Design and simulation of an energy storage system with batteries lead acid and lithium-ion for an electric vehicle: Battery vs. conduction cycle efficiency analysis. *IEEE Latin America Transactions*, 18(08), 1345-1352.

[8] Katuri, R., & Gorantla, S. (2020). Optimal performance of Lithium-Ion battery and ultra-capacitor with a novel control technique used in e-vehicles. *Journal of New Materials for Electrochemical Systems*, 23(2), 139-150.

[9] Zheng, C., Li, W., & Liang, Q. (2018). An energy management strategy of hybrid energy storage systems for electric vehicle applications. *IEEE Transactions on Sustainable Energy*, 9(4), 1880-1888.

[10] Shen, J., & Khaligh, A. (2015). A supervisory energy management control strategy in a battery/ultracapacitor hybrid energy storage system. *IEEE Transactions on transportation electrification*, 1(3), 223-231.

[11] Cao, J., & Emadi, A. (2011). A new battery/ultracapacitor hybrid energy storage system for electric, hybrid, and plug-in hybrid electric vehicles. *IEEE Transactions on power electronics*, 27(1), 122-132.

[12] Zhang, L., Ye, X., Xia, X., & Barzegar, F. (2020). A real-time energy management and speed controller for an electric vehicle powered by a hybrid energy storage system. *IEEE Transactions on Industrial Informatics*, 16(10), 6272-6280.

[13] Satoru Ohta (2023). Necessary Conditions and Empirical Observations for Rearrangeable Banyan-Type Networks. *WSEAS Transactions on Circuits and Systems*, vol.22, pp.180-194, https://doi.org/10.37394/23201.2023.22.21.

[14] Alexander Zemliak (2023). Analysis of Some Special Functions for a Problem of Optimization of Analog Circuits. *WSEAS Transactions on Circuits and Systems*, vol.22, pp.98-110, https://doi.org/10.37394/23201.2023.22.12.

[15] Khaldi Hamza, Mounir Hamid, Boulakhbar Mouaad (2022). A Review of Future Fuel Cell Electric Vehicles and Challenges Related to Morocco. *WSEAS Transactions on Power Systems,* vol.17, pp.339-353, https://doi.org/10.37394/232016.2022.17.34.

[16] Candidus U. Eya, Ayodeji Olalekan Salau, Sepiribo Lucky Braide, S. B. Goyal, Victor Adewale Owoeye, Oluwafunso Oluwole Osaloni (2022). Assessment of Total Harmonic Distortion in Buck-Boost DC-AC Converters using Triangular Wave and Saw-Tooth based Unipolar Modulation Schemes. *WSEAS Transactions on Power Systems.* vol.17, pp.324-338, https://doi.org/10.37394/232016.2022.17.33.

[17] X. Li and S. Wang (2021), "Energy management and operational control methods for grid battery energy storage systems," *in CSEE Journal of Power and Energy Systems*, vol. 7, no. 5, pp. 1026-1040.

[18] Yan, N., Zhong, Y., Li, X., Wang, Y., Su, L., Jiang, W., & Zhou, J. (2021). Energy management method of electricity heat hydrogen multi-coupling system for retired power battery echelon utilization in microgrids. *IEEE Transactions on Applied Superconductivity*, 31(8), 1-5.

[19] M. A. Izumida Martins, L. B. Rhode and A. B. D. Almeida (2022), "A Novel Battery Wear Model for Energy Management in Microgrids," *in IEEE Access*, vol. 10, pp. 30405-30413.

[20] S. Li, P. Zhao, C. Gu, J. Li, D. Huo and S. Cheng (2023), "Aging Mitigation for Battery Energy Storage System in Electric Vehicles," *in IEEE Transactions on Smart Grid*, vol. 14, no. 3, pp. 2152-2163.

Contribution of Individual Authors to the Creation of a Scientific Article (Ghostwriting Policy)

The authors equally contributed to the present research, at all stages from the formulation of the problem to the final findings and solution.

Sources of Funding for Research Presented in a Scientific Article or Scientific Article Itself

No funding was received for conducting this study.

Conflict of Interest

The authors have no conflicts of interest to declare.